Acid-Base Self-Assembly Chemistry and Hydrogen Bonding Interactions Resulting in the Formation of a Tetranuclear Aggregate Containing Four Crystallographically Non-Equivalent Fe^{III} Centers

Stefania Tanase,[a] Elisabeth Bouwman,[a] Gary J. Long,[b] Ahmed M. Shahin,[b] Allison M. Mills,[c] Anthony L. Spek,[c] and Jan Reedijk*[a]

Keywords: Iron / Pyrazole ligands / Hydroxo bridge / Mössbauer

The synthesis and characterization of a mononuclear iron(III) complex [Fe(Hphpz)Cl(CH_3OH)] (**1**) and a tetranuclear assembly of a bis(μ-hydroxo)-bridged dinuclear iron(III) complex [{Fe(Hphpz)$_2$(OH)}$_2$][Fe(Hphpz)$_3$]$_2$ (**2**) with the ligand 3(5)-methyl-5(3)-(2-hydroxyphenyl)pyrazole (H_2phpz) is reported. Compound **1** is converted into **2** in a methanol solution and in the presence of a base. The asymmetric unit of **2** consists of two independent [Fe(Hphpz)$_3$] molecules and one dinuclear complex [Fe(Hphpz)$_2$(OH)]$_2$ containing two crystallographically non-equivalent iron(iii) ions; the three units are linked by N–H···O and O–H···O hydrogen bonding and stacking interactions to form a cluster with an approximate C_2-symmetry. The Mössbauer spectra of [{Fe(Hphpz)$_2$-(OH)}$_2$][Fe(phpz)$_3$]$_2$ have been measured at 295 and 78 K and indicate the presence of four crystallographically distinct, but chemically similar iron(III) sites. The magnetic properties of this compound originate from the weak antiferromagnetic interaction between the Fe^{III} ions of the [Fe(phpz)$_2$(OH)]$_2$ dimer ($J = -2.8$ cm^{-1}).

Introduction

The chemistry of dinuclear iron(III) complexes bridged by carboxylato residues and/or by a single water-derived ligand (such as hydroxo or oxo) continues to be of great interest because of their implication in the active site of a number of metalloproteins, such as hemerytin (Hr),[1] ribonucleotide reductase (RR),[2] methane monooxygenase (MMO),[3] and purple acid phosphatase (PAPs).[4] At various stages of the enzymatic cycle, the type of the bridge and water-derived ligands may vary depending on the protein. The coordination spheres of the two iron centers play important roles in providing selective substrate binding, control of the iron oxidation states and stereochemical control of the intermediates in the enzymatic cycle. The functions performed by these metalloproteins and their significance have inspired a range of biomimetic studies, studies which suggest that bio-inspired catalytic oxidations might represent a valuable approach for the development of new and more environmentally friendly catalysts for industrial applications. Because spectroscopy plays a key complementary role in obtaining molecular-level insight into the catalytic mechanism that occurs at the active site of metalloproteins, the synthesis of small molecule model compounds has remained a challenging field.

As part of a programme of synthesizing dinuclear iron complexes which model the active sites of metalloproteins, we have chosen to work with nitrogenous and oxygenous ligands and, in particular, with pyrazole-containing ligands.[5] Pyrazole-containing ligands provide an interesting alternative to the often used pyridine ligands for the design of model complexes that can mimic active sites containing imidazole groups from histidine bound to an iron center.[6,7] Especially the lower pK_a values of the pyrazoles and the availability of an acid N−H group as possible hydrogen-bond donor, provide an interesting possibility for new structural features. So, these ligands might even be preferred in the field of biomimetic chemistry, both because they are good structural analogues for the size and electronic properties of histidine and because of their relative ease of preparation as compared to imidazole ligands. In this regard and because of the occurrence of tyrosinase radicals in metalloproteins involved in oxygen-dependent enzymatic radical catalysis,[8] we have been interested in the assembly of discrete diiron(III) cores from 3(5)-methyl-5(3)-(2-

[a] Leiden Institute of Chemistry, Gorlaeus Laboratories, Leiden University
P. O. Box 9502, 2300 RA Leiden, The Netherlands
Fax: + 31 71-527-4671
E-mail: reedijk@chem.leidenuniv.nl
[b] Department of Chemistry, University of Missouri-Rolla, Rolla, MO 65409-0010, USA
[c] Bijvoet Center for Biomolecular Research, Utrecht University, Padualaan 8, 3584 CH Utrecht, The Netherlands

Supporting information for this article is available on the WWW under http://www.eurjic.org or from the author.

  DOI: 10.1002/ejic.200400609

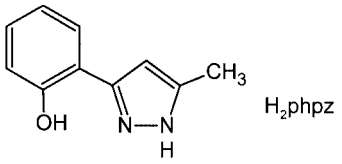

Scheme 1

hydroxyphenyl)pyrazole (H_2phpz, Scheme 1) and simple donors, such as hydroxide, formate, acetate, and benzoate. We report herein the synthesis, structural, spectroscopic and magnetic characterization of $[\{Fe(Hphpz)_2(OH)\}_2][Fe(phpz)_3]_2$, a compound which contains a $Fe_2(\mu\text{-}OH)_2$ core and is extensively stabilized by hydrogen bonding and stacking interactions between the lattice components.

Results and Discussion

Synthesis and Characterization of Iron Complexes of H_2phpz

The procedure for synthesizing the H_2phpz ligand[10] has been reported previously; for the mono-anionic Hphpz, only the mononuclear complex $[Fe(Hphpz)(MeOH)_2](NO_3)$ has so far been reported.[9] In the present study, the reaction of H_2phpz with $Fe(NO_3)_3$, and with other iron(III) salts in various solvents has been extensively investigated. However, elemental analysis and ligand field spectra reveal that mixtures of compounds are obtained in all cases. Therefore, a more specific systematic study had to be undertaken. The reaction of the ligand H_2phpz with $FeCl_2$ (2:1) in the presence of two equiv. of base in methanol leads to a dark purple crystalline product with the tentative formula $[Fe(Hphpz)_2Cl(MeOH)]$ (**1**) as suggested by elemental analysis (Scheme 2). The positive ion mass spectrum of a fresh solution of **1** in either methanol or CH_2Cl_2 exhibits a prominent signal at $m/z = 433$ (relative intensity $I = 100\%$ in the range $m/z = 200-1000$). This signal matches very well with the calculated isotopic distribution for $[Fe(Hphpz)_2(MeOH)]^+$. The effective magnetic moment of **1** at room temperature (5.84 μ_β) is close to the spin-only value expected for a high-spin iron(III) center ($S = {}^5/_2$, $\mu_{eff} = 5.92\ \mu_\beta$); the variable temperature solid-state magnetic susceptibility of **1** has been investigated in the range 5−300 K and it displays strict Curie−Weiss behaviour consistent with the presence of an isolated paramagnetic iron(III) ion. No single crystals were obtained however.

Coordination of 3(5)-methyl-5(3)-(2-hydroxyphenyl)pyrazole with the iron(III) ion is indicated in the infrared spectrum by a shift of the ν_{C-O} stretch from 1654 cm^{-1} in the free ligand to 1599 cm^{-1} in complex **1** and of the $\nu_{C=N}$ stretch from 1636 cm^{-1} in the free ligand to 1557 cm^{-1} in the complex. A sharp peak observed at 3259 cm^{-1} can be assigned to the ν_{N-H} stretch of the pyrazole ring. The absence of any absorption in the range 3300−3600 cm^{-1} indicates that the phenolic proton is lost on coordination.

The main feature of the UV/Vis spectrum of **1** in the solid state is a low-energy band with a maximum at 568 nm that gives rise to the purple colour and which is ascribed to the charge-transfer transition from the p_π orbitals of the phenolic oxygens to the d_π* orbitals of the iron(III) ions.[9,11] A second charge-transfer band occurs at 369 nm and has been assigned to a $p_\pi \rightarrow d_\sigma$* type transition.[11] Electronic absorption spectra of **1** have also been recorded in methanol and dichloromethane, and both show spectroscopic features that are similar to that in the solid state consisting of two absorption bands with maxima at 359 nm and 547 nm, respectively and it suggests that the chloride ion is not replaced by methanol.

The cyclic voltammogram of **1** recorded at room temperature in CH_2Cl_2 shows an irreversible cathodic wave at 0.83 V vs. Ag/AgCl, which is ascribed to the reduction of iron(III) to iron(II). The relatively high reduction potential suggests that **1** is stabilized by the coordination of the chloride anion. This stabilization is also confirmed by the absence of any oxidation peak when scanning the potential up to 1.2 V, a potential at which free chloride ions may be detected.

When a purple-colored methanol solution of **1** is stored in a closed inert atmosphere it gradually changes to red over a number of days. Ligand field spectra would suggest that the new species is a mixture of $[Fe(Hphpz)_2Cl(MeOH)]$, $[Fe(Hphpz)_2(OH)]_2$ and $[Fe(Hphpz)_3]$. Addition of 2 equiv. of base to a fresh methanol solution of **1** results in the immediate appearance of an intense red coloration, accompanied by significant spectroscopic changes (Figure 1). The absorption maximum at 490 nm suggest the presence of a bis(μ-hydroxo) dimer.[12] The function of the added base appears to be to provide the medium required for the formation of the $Fe_2(\mu\text{-}OH)_2$ core. Vapor diffusion of ethyl acetate into this solution yields a red microcrystalline solid, for which elemental analysis indicates the formula $[\{Fe(Hphpz)_2(OH)\}_2][Fe(Hphpz)_3]_2$ (**2**). Thus, it appears that compound **2** is a decomposition product of **1**. Although we were unsuccessful in growing crystals large enough to carry out an X-ray structural study of **1**, we were successful in growing crystals of **2**. The yield of compound **2** has been optimized via acid-base self assembly chemistry (Scheme 2), by mixing

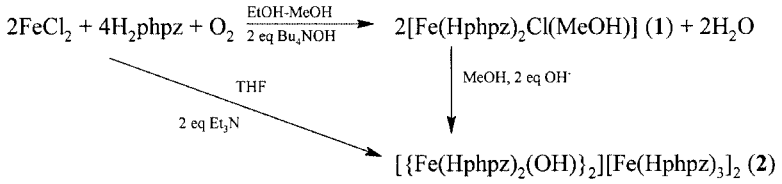

Scheme 2. Reaction pathways for the synthesis of compounds **1** and **2**

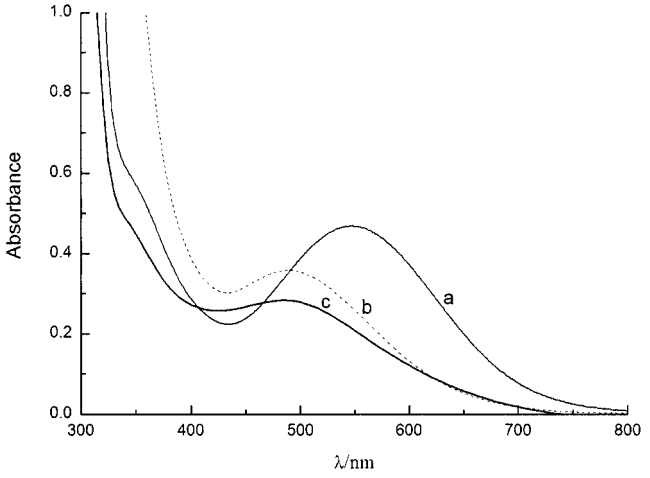

Figure 1. UV/Vis spectra of a methanol solution of $[Fe(Hphpz)_2Cl(MeOH)]$ (a), after the addition of 2 equiv. of Bu_4NOH to **1** (b), and $[\{Fe(Hphpz)_2(OH)\}_2][Fe(Hphpz)_3]_2$ redissolved in methanol (c)

$FeCl_2{\cdot}4H_2O$ with H_2phpz under air in the presence of triethylamine as base.

The infrared spectrum of **2** exhibits the bands expected for the ligand Hphpz and it is similar to that of the compound **1**. Unfortunately, it is not possible to definitely identify the Fe−O−Fe vibrational bands, because of the complexity of the infrared spectrum in the 500−800 cm^{-1} range. The ligand field spectrum of **2** displays the features typical of bis(μ-hydroxo)-bridged iron(III) compounds: an intense absorption band at 495 nm with a lower energy shoulder at 586 nm, bands that may be assigned to ligand-to-iron(III) charge-transfer transitions.[13] A weak-intensity absorption band that occurs at 997 nm is attributed to the d-d transitions involving forbidden states of the high-spin iron(III) ion.[14]

X-ray Crystal Structure of $[\{Fe(Hphpz)_2(OH)\}_2][Fe(Hphpz)_3]_2$

Perspective views of the molecular entities of **2** are shown in Figure 2 along with the atom-labeling scheme. The asymmetric unit of **2** contains two independent *mer*-$[Fe(Hphpz)_3]$ molecules and one dinuclear complex $[Fe(Hphpz)_2(OH)]_2$. Selected bond lengths and angles pertaining to the iron(III) coordination spheres are given in Table 1.

Each of the two independent $[Fe(Hphpz)_3]$ molecules consists of an iron(III) ion coordinated to three $phpz^-$ ligands (Figure 2, a and b). The distorted octahedral-based FeN_3O_3 chromophores both have a meridional (*mer*) configuration. The bond lengths and angles at the iron center are similar in both entities and indicate an extensive deviation from octahedral symmetry (Table 1, Supplementary material). The largest deviations from ideal octahedral symmetry are observed for the *trans* O21−Fe1−O61 = 162.10(14)° and O81−Fe2−O121 = 161.67(15)° angles. The least-square phenyl rings and pyrazole rings in the $Hphpz^-$ ligand containing N32 and N92 nitrogen atoms make dihedral angles of 8.2(3) and 2.1(3)°. Although a planar molecule is expected, the $Hphpz^-$ ligand may also bind in a twisted conformation because the conjugation of the phenyl−pyrazole bond is flexible. Due to the aromaticity of the pyrazole ring the lone pair of the nitrogen, and therefore the coordinated metal ion all are expected to lie in a nearly perfect plane. In the case of the pyrazole ring containing N32 and the one containing N92, however, the iron atoms lie 0.8−1.0 Å above the least-squares plane of the pyrazole ring. This implies that the pyrazole ring is bound to the iron atoms in a rather acute angle of 19.41° and 20.59°. The hydrogen bonding interactions from N−H to a neighboring oxygen atoms and the π-π interactions clearly enforce the deviation from the planarity of distorted $Hphpz^-$ ligands (see below). The $Fe-N_{pz}$ and $Fe-O_{ph}$ bond lengths are very similar to those found in the dinuclear species $[Fe(Hphpz)_2(OH)]_2$.

The dinuclear $[Fe(Hphpz)_2(OH)]_2$ unit contains two crystallographically non-equivalent iron(III) ions that are bridged by two hydroxyl groups (Figure 2, c). The nitrogen and oxygen donors of two molecules of the H_2phpz ligand in its mono-dehydronated form ($Hphpz^-$) occupy four coordination sites of each iron(III) ion. At Fe3 the nitrogen donors of the two ligands are mutually *trans*, whereas at Fe4 they are positioned *cis* with respect to one another. The two remaining sites are filled by the bridging hydroxyl ions. Therefore, each iron(III) ion has a N_2O_4 donor set in a distorted octahedral coordination geometry. All *cis* and *trans* angles deviate from 90 and 180°; in particular, the angles N192−Fe4−O210 = 162.48(14)° and N172−Fe4−O211 = 162.56(14)° are considerably kinked. In the four-membered $Fe_2(\mu\text{-}OH)_2$ core, the two metal centers are separated by 3.1492(9) Å and have two slightly different bridging angles of Fe3−O210−Fe4 = 105.45(14)° and Fe3−O211−Fe4 104.97(14)°. Each of the hydroxyl ions bridges the metal centers asymmetrically; the Fe3−OH distances are somewhat shorter than those for Fe4, which may be related to the *trans* effect of the nitrogen donors and to the steric requirements of the Hphpz ligands. All of the $Fe^{III}-\mu$-OH bond lengths, as well as the Fe−OH−Fe bridge angles, are in the range of those observed for similar $Fe_2(\mu\text{-}OH)_2$ complexes.[15−18] The $Fe-N_{pz}$ and $Fe-O_{ph}$ bond lengths are also comparable to those reported for related complexes.[9,19]

An interesting feature of the crystal structure of **2** is the presence of multiple intra- and intermolecular hydrogen bonds, as well as intermolecular π···π stacking interactions, interactions which play an important role in the stabilization of the observed molecular configuration (Figure 3 and Table S1 in the Supporting Information). Two strong intramolecular N−H···O hydrogen bonds (N−H···O = 2.803 Å) link $Hphpz^-$ ligands on different iron centres in the $[Fe(Hphpz)_2(OH)]_2$ unit. In each of the $[Fe(Hphpz)_3]$ molecules, two intramolecular N−H···O hydrogen bonds are established between two of the anionic $Hphpz^-$ ligands. The third anionic $phpz^-$ molecule of each mononuclear entity is involved in two intermolecular N−H···O hydrogen bonds with $Hphpz^-$ ligands of the dinuclear

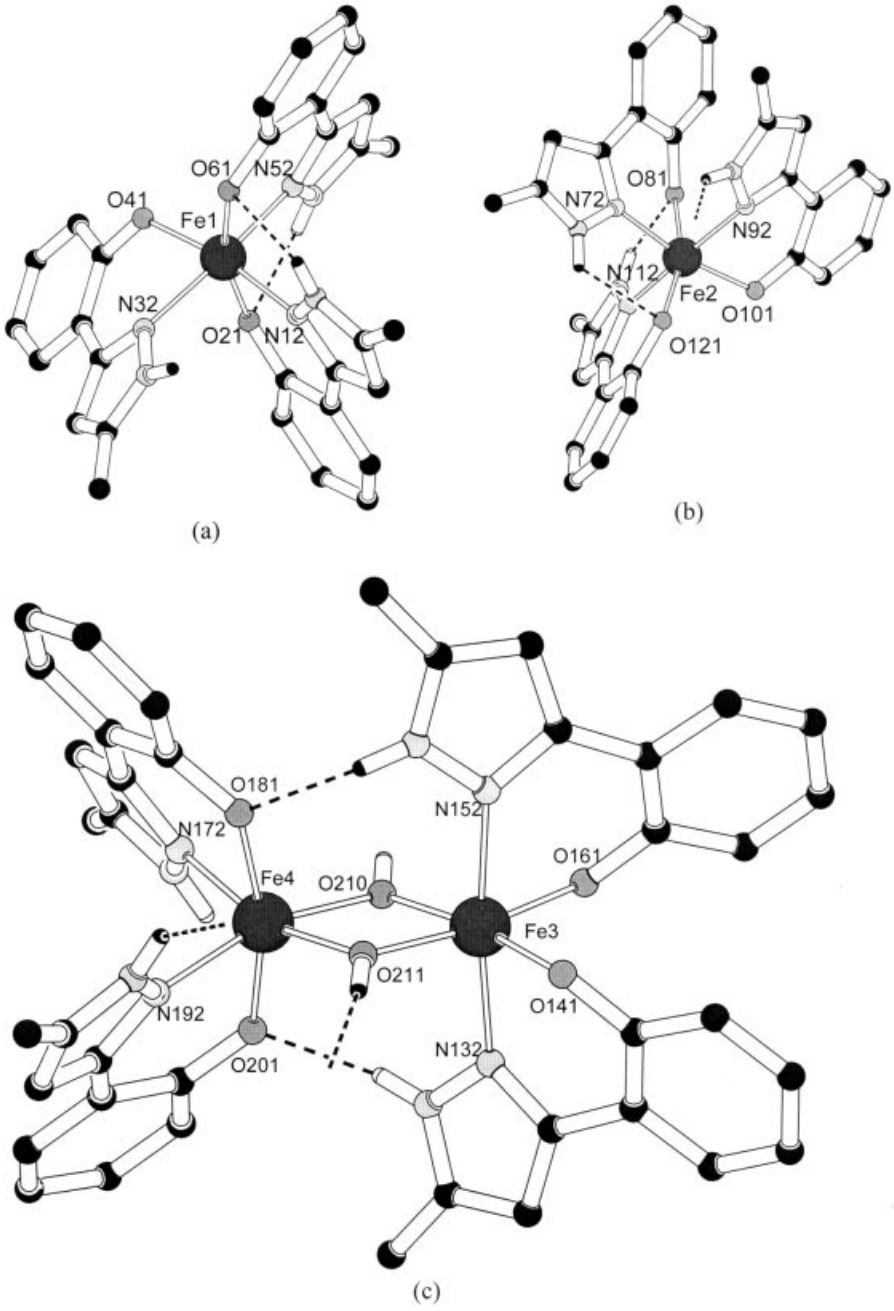

Figure 2. Pluton projections and labeling scheme of the three molecules of the asymmetric unit of $[\{Fe(Hphpz)_2(OH)\}_2][Fe(Hphpz)_3]_2$ (**2**) including the hydrogen bond interactions

$[Fe(Hphpz)_2(OH)]_2$. Two strong O−H···O hydrogen bonds occur between the hydroxo-bridges of $[Fe(Hphpz)_2(OH)]_2$ and the O donor of one $Hphpz^-$ ligand from each $[Fe(Hphpz)_3]$ monomer. Thus, the three molecules are linked by N−H···O and O−H···O hydrogen bonding interactions to form a tetranuclear assembly with approximate C_2-symmetry. Several intermolecular π···π stacking interactions involving aromatic rings of the of the $Hphpz^-$ ligands of the three iron complexes further reinforce the tetranuclear assembly (Table S2 in the Supporting Information). An additional inter − tetranuclear assembly π···π interaction occurs between peripheral pyrazole rings of inversion-related tetranuclear assemblies. The optimization of these packing interactions leads to $Hphpz^-$ ligand conformations varying from nearly planar to considerably twisted; the dihedral angles between the phenyl and pyrazole ring planes within the ligands range from 1.6(3) to 23.0(4)°. In the three-dimensional structure of $[\{Fe(Hphpz)_2(OH)\}_2]$-$[Fe(Hphpz)_3]_2$, the assemblies are separated by large voids filled with disorded THF solvent molecules.

Mössbauer Spectroscopic Results

To study the four different species in more detail, Mössbauer spectroscopy was applied with fitting pro-

Table 1. Selected bond lengths (Å) and angles (°) for $[\{Fe(Hphpz)_2(OH)\}_2][Fe(Hphpz)_3]_2$

Bond lengths			
Fe1−O21	1.942(3)	Fe3−O141	1.990(3)
Fe1−O41	1.942(3)	Fe3−O161	1.986(3)
Fe1−O61	1.960(3)	Fe3−O210	1.968(3)
Fe1−N12	2.099(4)	Fe3−O211	1.979(3)
Fe1−N32	2.156(4)	Fe3−N132	2.117(4)
Fe1−N52	2.109(4)	Fe3−N152	2.118(4)
Fe2−O81	1.952(3)	Fe4−O181	1.971(3)
Fe2−O101	1.945(3)	Fe4−O201	1.968(3)
Fe2−O121	1.941(3)	Fe4−O210	1.990(3)
Fe2−N72	2.122(5)	Fe4−O211	1.991(3)
Fe2−N92	2.157(4)	Fe4−N172	2.119(4)
Fe2−N112	2.109(4)	Fe4−N192	2.134(4)
Bond angles			
O21−Fe1−O41	94.67(13)	O141−Fe3−O161	94.14(13)
O21−Fe1−O61	162.12(13)	O141−Fe3−O210	169.71(14)
N32−Fe1−N52	172.32(15)	O141−Fe3−O211	95.33(13)
N12−Fe1−N32	88.30(15)	O161−Fe3−O211	169.88(12)
O41−Fe1−N32	81.43(13)	O161−Fe3−N152	83.20(13)
O61−Fe1−N32	102.08(13)	O210−Fe3−N152	92.94(13)
O41−Fe1−N12	169.61(14)	N132−Fe3−N152	173.50(15)
O61−Fe1−N52	82.75(13)	O210−Fe3−O211	75.16(13)
O81−Fe2−O101	95.75(15)	O181−Fe4−O201	165.28(12)
O81−Fe2−O121	161.65(15)	O181−Fe4−O210	104.84(12)
O121−Fe2−N92	102.2(14)	O181−Fe4−O211	86.72(12)
N92−Fe2−N112	172.22(16)	O201−Fe4−O211	105.29(12)
O101−Fe2−N92	80.88(14)	O210−Fe4−O211	74.42(13)
O81−Fe2−N72	82.87(17)	O210−Fe4−N192	162.48(14)
O101−Fe2−N72	167.15(16)	N172−Fe4−N192	99.16(15)
N72−Fe2−N112	99.19(16)	O211−Fe4−N172	162.57(14)

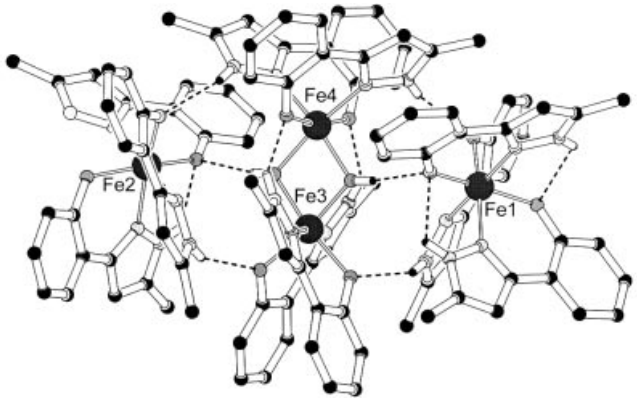

Figure 3. View of **2** showing the hydrogen-bonded network. Hydrogen atoms not involved in hydrogen bonding are omitted for clarity

cedures. The Mössbauer spectra of $[\{Fe(Hphpz)_2(OH)\}_2][Fe(Hphpz)_3]_2$ measured at 295 and 78 K are shown in Figure 4. As might be expected for a compound containing four crystallographically distinct, but chemically similar iron sites, the observed spectra do not show spectral resolution of the four different iron sites. Because of the four crystallographically different iron sites found in $[\{Fe(Hphpz)_2(OH)\}_2][Fe(Hphpz)_3]_2$, the Mössbauer spectra have been fitted with four symmetric quadrupole doublets whose relative areas were constrained to 25 percent each; the resulting hyperfine parameters are given in Table 2.

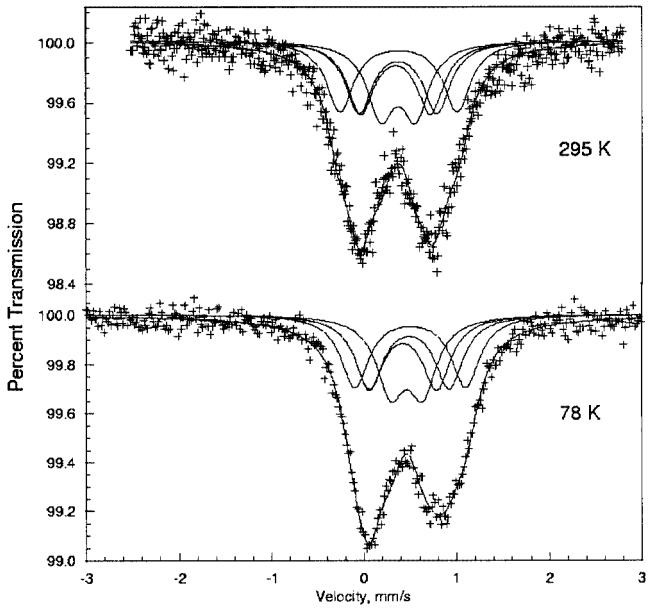

Figure 4. The Mössbauer spectra of **2** obtained at 78 K and 295 K together with the fits for four different species

Table 2. Mössbauer spectral hyperfine parameters of $[\{Fe(Hphpz)_2(OH)\}_2][Fe(Hphpz)_3]_2$

T [K]	δ[a] [mm/s]	ΔE_Q [mm/s]	Γ [mm/s]	Area [%]	Site assignment[b]
295	0.37	0.38	0.36	25	Fe(3)
	0.33	0.74	0.36	25	Fe(1)
	0.38	0.85	0.36	25	Fe(2)
	0.38	1.27	0.36	25	Fe(4)
average	0.365	0.81	0.36	−	
78	0.46	0.35	0.37	25	Fe(3)
	0.42	0.73	0.37	25	Fe(1)
	0.49	0.86	0.37	25	Fe(2)
	0.50	1.19	0.37	25	Fe(4)
average	0.47	0.78	0.37	−	

[a] The isomer shifts are given relative to room temperature α-iron foil. [b] Based on the degree of the octahedral distortions.

It should be noted that the 78 K spectrum shown in Figure 4 was obtained over an ca. ±5 mm/s range in order to detect the presence of any high-spin iron(II) spectral impurities. As expected none was observed and, as a consequence, the 295 K spectrum was obtained over an ca. ±2.5 mm/s range under different spectrometer geometric and electronic conditions. This difference accounts for the unexpected increase in the percentage transmission observed upon warming from 78 to 295 K and may also account for the small, but unexpected, increase in the quadrupole splitting observed upon warming.

Although the fits depicted in Figure 4 may not be unique, the average values of the hyperfine parameters are characteristic of $[\{Fe(Hphpz)_2(OH)\}_2][Fe(Hphpz)_3]_2$ and are typical of those expected of iron(III) in a distorted octahedral coordination environment.[5,20−22] In an attempt to assign

the different spectral components shown in Figure 4 the average bond angle distortion parameter, d, as defined[23] by

$$d = \frac{100}{n} \bullet \sum_{i=1}^{n} \frac{|a_i - a_m|}{a_m},$$

where n is the number of bonds, a_m is the mean angle, and a_i is an individual bond angle, has been calculated for each of the four different iron sites. The resulting bond angle distortions are 6.53, 7.09, 5.17, and 8.33% for sites Fe(1) to Fe(4), respectively. Because the quadrupole splitting observed at an iron(III) site will increase with increasing distortion of the coordination environment and hence the distortion of the octahedral bond angles, these parameters were used to make the assignments of the sites given in Table 2. However, it should be noted that these assignments are tentative, as the fits may not be unique.

Magnetic Properties

The variable temperature solid-state magnetic susceptibility of complex **2** is shown in the form of χ_m versus T and μ_{eff} versus T plots (Figure 5). The effective magnetic moment decreases as the temperature is lowered from 300 to 5 K. This variation indicates an overall antiferromagnetic behaviour for compound **2**. The temperature dependence of χ_m could be simulated by using the Van Vleck equation derived from the Heisenberg exchange Hamiltonian for two interacting spins $S_1 = S_2 = {}^5/_2$, modified in order to take into account the two isolated Fe^{III} ions.[24] The temperature-independent paramagnetism (TIP = $400 \cdot 10^{-6}$ $cm^3 \cdot K \cdot mol^{-1}$ for each iron ion) was taken into account. Using this approach, the best fit parameters were $J = -2.8$ cm^{-1}, $g = 2.03$. The exchange coupling parameter, J, is known to have values between -5 and -11 cm^{-1} in the case of bis(μ-hydroxo)-bridged iron(III) complexes and the low electron density of the hydroxo-bridge is likely to be responsible for the observed weak antiferromagnetic coupling.[15,25] In the present case, the remarkable dissymmetry of the $Fe_2(\mu\text{-}OH)_2$ core geometry accounts for the weaker antiferromagnetic coupling, as compared with related bis(μ-hydroxo)-bridged iron(III) compounds.

Conclusion

Two iron complexes of the ligand 3(5)-methyl-5(3)-(2-hydroxyphenyl)pyrazole, namely $[Fe(Hphpz)_2Cl(MeOH)]$ (**1**) and $[\{Fe(Hphpz)_2(OH)\}_2][Fe(Hphpz)_3]_2$ (**2**), have been synthesized and characterized by various spectroscopic measurements. Compound **2**, which appears to be a decomposition product of **1** was structurally characterized by X-ray diffraction; its asymmetric unit contains two independent $[Fe(Hphpz)_3]$ molecules and one dinuclear complex $[Fe(Hphpz)_2(OH)]_2$ with two crystallographically nonequivalent iron(III) ions. The remarkable dissymmetric dinuclear $[Fe(Hphpz)_2(OH)]_2$ unit is highly stabilized through π donation of the OH^- bridge and through N−H···O and O−H···O hydrogen bonds. Further attempts to isolate (μ-oxo)(μ-carboxylato)diiron(III) complexes based on $[Fe(Hphpz)_2]^+$ units are underway. The influence of different pyrazole derivatives on the stability of the $Fe_2(OH)_2$ core will also be investigated.

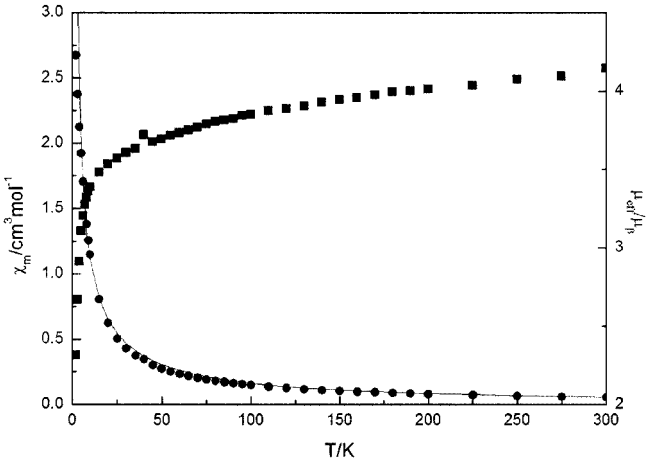

Figure 5. Plots of χ_m and μ_{eff} vs. temperature for compound **2**: (dots) experimental values; (−) calculated values for $J = -2.8$ cm^{-1} and $g = 2.03$

Experimental Section

General Remarks: All chemicals were of reagent grade, and were used as received. 3(5)-methyl-5(3)-(2-hydroxyphenyl)pyrazole (H_2phpz) was prepared by condensation of hydrazine and salicoylacetone as reported previously.[10] All experiments were carried out in air, unless stated otherwise.

Physical Measurements: Elemental analyses for C, H, and N were performed on a Perkin−Elmer 2400 Series II analyzer. Infrared spectra (4000−300 cm^{-1}) were recorded on a Perkin−Elmer Paragon 1000 FTIR spectrometer equipped with a Golden Gate ATR device, using the reflectance technique. UV/Vis spectra were obtained on a Perkin−Elmer Lambda 900 spectrophotometer using the diffuse reflectance technique, with MgO as a reference. Magnetic susceptibility measurements (5−300 K) were carried out at 0.1 T using a Quantum Design MPMS-5 5T SQUID magnetometer. Data were corrected for magnetization of the sample holder and for diamagnetic contributions, which were calculated from the Pascal constants. Mössbauer spectra were measured on a constant-acceleration spectrometer that utilized a room temperature rhodium matrix cobalt-57 source and was calibrated at room temperature with α-iron foil.

$[Fe(Hphpz)_2Cl(MeOH)]$ (1) was synthesized by adding an ethanolic solution containing 3(5)-methyl-5(3)-(2-hydroxyphenyl)pyrazole (0.322 g, 2 mmol) and Bu_4NOH (2 mmol, solution in methanol) to an ethanolic solution of $FeCl_2 \cdot 4H_2O$ (0.198 g, 1 mmol) and stirring for one hour. The resulting dark purple precipitate was collected by filtration, washed with diethyl ether and dried under vacuum. Yield: 72%. $C_{21}H_{22}ClFeN_4O_3$ (469.73): calcd. C 53.70, H 4.72, N 11.93; found C 54.04, H 4.51, N 12.29. IR ($\tilde{\nu}$/cm^{-1}): 3259 s, 2971 m, 2889 m, 1599 m, 1557 s, 1456 m, 1310 s, 1243 m, 1119 m, 1063 m, 982 w, 865 s, 784 s, 747 s, 656 m, 628 m, 583 m, 553 s, 438 m, 386 m. UV/Vis/NIR, $\lambda_{?max}$/nm (ε/m$M^{-1}cm^{-1}$): 264, 369, 568; 359 (3.9), 547(3.5) in methanol solution.

$[\{Fe(Hphpz)_2(OH)\}_2][Fe(Hphpz)_3]_2$ (2) was obtained by slow diffusion of hexane into a tetrahydrofuran solution containing

$FeCl_2 \cdot 4H_2O$ (0.397 g, 2 mmol) and 3(5)-methyl-5(3)-(2-hydroxyphenyl)pyrazole (0.644 g, 4 mmol) in the presence of 4 equiv. of triethylamine. The resulting red crystals were collected by filtration, washed with diethyl ether and dried under vacuum. Yield: 65% based on iron. $C_{100}H_{92}Fe_4N_{20}O_{12}$ (1989.34): calcd. C 60.38, H 4.66, N 14.08; found C 60.04, H 4.51, N 14.29. IR ($\tilde{\nu}$/cm^{-1}): 3183 m, 2918 m, 2817 m, 1597 m, 1557 m, 1457 s, 1290 m, 1254 m, 1117 m, 1040 m, 972 w, 848 s, 788 m, 751 s, 602 m, 563 m, 481 m. UV/Vis/NIR, $\lambda_{?max}$/nm (ε/mM^{-1}cm^{-1}): 255, 311, 495, 997; 490(3.2) in methanol solution.

X-ray Crystallographic Study: Intensity data for a single crystal of **2** were collected using Mo-K_α radiation (λ = 0.71073 Å) on a Nonius KappaCCD diffractometer. A correction for absorption was considered unnecessary. The structure was solved by automated Patterson methods using SHELXS-97[26] and was refined on F^2 by least-squares procedures using SHELXL-97.[27] The crystal structure contains voids (799.3 A^3/unit cell) filled with disordered THF solvent molecules. Their contribution to the structure factors was ascertained using PLATON/SQUEEZE (206 e/unit cell).[28] All non-hydrogen atoms were refined with anisotropic displacement parameters. The hydroxyl hydrogen atoms were positively identified in a difference Fourier map, and their positions were refined with the restraint that the O−H distances be similar. All other hydrogen atoms were constrained to idealized geometries and allowed to ride on their carrier atoms. The hydrogen atoms of some methyl groups are disordered over two sets of positions. All hydrogen atoms were refined with an isotropic displacement parameter related to the equivalent displacement parameter of their carrier atoms. Structure validation and molecular graphics preparation were performed with the PLATON package.[28] CCDC-244433 contains the supplementary crystallographic data for this paper. These data can be obtained free of charge at www.ccdc.cam.ac.uk/conts/retrieving.html [or from the Cambridge Crystallographic Data Centre, 12 Union Road, Cambridge CB2 1EZ, UK; Fax: +44-1223-336-033; E-mail: deposit@ccdc.cam.ac.uk].

Acknowledgments

This work was financially supported by the Dutch Economy, Ecology, Technology (EET) programme, a joint programme of the Ministry of Economic Affairs, the Ministry of Education, Culture and Science, and the Ministry of Housing, Spatial Planning and the Environment. We would like to acknowledge Dr. R. Hage (Unilever, The Netherlands) for useful discussions.

[1] R. E. Stenkamp, *Chem. Rev.* **1994**, *94*, 715−726.
[2] D. T. Logan, X. D. Su, A. Aberg, K. Regnstrom, J. Hajdu, H. Eklund, P. Nordlund, *Structure* **1996**, *4*, 1053−1064.
[3] A. C. Rosenzweig, C. A. Frederick, S. J. Lippard, P. Nordlund, *Nature* **1993**, *366*, 537−543.
[4] T. Klabunde, N. Sträter, B. Krebs, H. Witzel, *FEBS Lett.* **1995**, *367*, 56−60.
[5] S. Tanase, E. Bouwman, G. J. Long, A. M. Shahin, R. de Gelder, A. M. Mills, A. L. Spek, J. Reedijk, *Polyhedron*, manuscript submitted.
[6] R. Mukherjee, *Coord. Chem. Rev.* **2000**, *203*, 151−218.
[7] H. Toftlund, *Coord. Chem. Rev.* **1989**, *94*, 67−108.
[8] R. H. Holm, P. Kennepohl, E. I. Solomon, *Chem. Rev.* **1996**, *96*, 2239−2314.
[9] E. W. Ainscough, A. M. Brodie, J. E. Plowman, K. L. Brown, A. W. Addison, A. R. Gainsford, *Inorg. Chem.* **1980**, *19*, 3655−3663.
[10] A. W. Addison, P. J. Burke, *J. Heterocyclic Chem.* **1981**, *18*, 803−805.
[11] B. P. Gaber, V. Miskowski, T. G. Spiro, *J. Am. Chem. Soc.* **1974**, *96*, 6868−6873.
[12] E. J. Enemark, T. D. P. Stack, *Inorg. Chem.* **1996**, *35*, 2719−2720.
[13] J. A. Bertrand, P. G. Eller, *Inorg. Chem.* **1974**, *13*, 927−934.
[14] A. B. P. Lever, *Inorganic Electronic Spectroscopy*, Elsevier Science B. V., Amsterdam, **1986**.
[15] E. I. Solomon, T. C. Brunold, M. I. Davis, J. N. Kemsley, S. K. Lee, N. Lehnert, F. Neese, A. J. Skulan, Y. S. Yang, J. Zhou, *Chem. Rev.* **2000**, *100*, 235−349.
[16] V. L. MacMurdo, H. Zheng, L. Que, *Inorg. Chem.* **2000**, *39*, 2254−2255.
[17] D. Lee, J. Du Bois, D. Petasis, M. P. Hendrich, C. Krebs, B. H. Huynh, S. J. Lippard, *J. Am. Chem. Soc.* **1999**, *121*, 9893−9894.
[18] D. W. Lee, S. J. Lippard, *J. Am. Chem. Soc.* **1998**, *120*, 12153−12154.
[19] S. K. Dutta, K. K. Nanda, U. Florke, M. Bhadbhade, K. Nag, *J. Chem. Dalton-Trans.* **1996**, 2371−2379.
[20] G. J. Long, J. T. Wrobleski, R. V. Thundathil, D. M. Sparlin, E. O. Schlemper, *J. Am. Chem. Soc.* **1980**, *102*, 6040−6046.
[21] W. M. Reiff, G. J. Long, W. A. Baker, *J. Am. Chem. Soc.* **1968**, *90*, 6347−6351.
[22] J. A. Bertrand, J. L. Breece, A. R. Kalyanaraman, G. J. Long, W. A. Baker, *J. Am. Chem. Soc.* **1970**, *92*, 5233−5234.
[23] B. Renner, G. Lehmann, *Z. Krist.* **1986**, *175*, 43−59.
[24] O. Kahn, *Molecular Magnetism*, VCH Publishers, New York, **1993**.
[25] W. Rudiger, S. Ostrovsky, K. Griesar, W. Haase, *Inorg. Chim. Acta* **2001**, *326*, 78−88.
[26] G. M. Sheldrick, *SHELXS-97. Program for Crystal Structure solution*, University of Göttingen, Germany, **1997**.
[27] G. M. Sheldrick, *SHELXL-97. Program for Crystal Structure refinement*, University of Göttingen, Germany, **1997**.
[28] A. L. Spek, *PLATON, A Multi-purpose Crystallographic Tool*, Utrecht University, The Netherlands, **2003**.

Received July 14, 2004
Early View Article
Published Online October 14, 2004

